

## RESEARCH ARTICLE

# Voltages and resistances of the anterior Malpighian tubule of *Drosophila melanogaster*

Klaus W. Beyenbach

## ABSTRACT

The small size of Malpighian tubules in the fruit fly *Drosophila melanogaster* has discouraged measurements of the transepithelial electrical resistance. The present study introduces two methods for measuring the transepithelial resistance in isolated *D. melanogaster* Malpighian tubules using conventional microelectrodes and PClamp hardware and software. The first method uses three microelectrodes to measure the specific transepithelial resistance normalized to tubule length or luminal surface area for comparison with resistances of other epithelia. The second method uses only two microelectrodes to measure the relative resistance for comparing before and after effects in a single Malpighian tubule. Knowledge of the specific transepithelial resistance allows the first electrical model of electrolyte secretion by the main segment of the anterior Malpighian tubule of *D. melanogaster*. The electrical model is remarkably similar to that of the distal Malpighian tubule of *Aedes aegypti* when tubules of *Drosophila* and *Aedes* are studied *in vitro* under the same experimental conditions. Thus, despite 189 millions of years of evolution separating these two genera, the electrophysiological properties of their Malpighian tubules remains remarkably conserved.

**KEY WORDS:** Cable analysis, Diuretics, Electrogenic transport, Epithelial electrophysiology, Fluid secretion, Kinins

## INTRODUCTION

The transepithelial electrical resistance is easily measured in a planar epithelium as the ratio of the transepithelial voltage deflection consequent to a transepithelial current pulse at uniform current density (Ohm's law). The current density cannot be uniform in a tubular epithelium unless a wire is passed through the tubule lumen, which so far has been accomplished only once in a renal epithelium. Taking advantage of the large size of the renal proximal tubule of the aquatic salamander *Necturus maculosus*, Spring and Paganelli (1972) were able to pass a platinized tungsten wire through the tubule lumen to measure a specific transepithelial resistance ( $R_t$ ) of  $43 \Omega \text{ cm}^2$ . All other measurements of  $R_t$  in tubular epithelia are grounded in cable theory (Taylor, 1963), which models the tubule as an electrical cable. The fluid in the tubule lumen is considered the conductive cable core and the surrounding epithelial cells are considered the insulator. Current is passed into the tubule lumen from a point source (microelectrode), and the transepithelial voltage deflections are recorded with microelectrodes at other points in the tubule lumen. The decay of the injected current along the

length of the tubule depends on (1) the tubule geometry (length and lumen diameter), (2) the resistivity of the fluid occupying the tubule lumen and (3) the electrical properties of the epithelial cells, i.e. the transepithelial resistance.

The tubule may be modelled as a cable of finite length or infinite length. In the finite-length model, the two ends of the tubule are electrically isolated from the peritubular medium, defining the tubule length as in isolated perfused renal tubules (Burg et al., 1966; Helman, 1972). When the electrical isolation of the tubule ends is not possible, the tubule is considered a cable of infinite length (Boulpaep and Giebisch, 1978; Frömter, 1986; Hegel et al., 1967). For both models, variations of single- and double-barreled microelectrodes and measuring circuits have been employed to determine the cable parameters. In the present study, I introduce the use of three conventional microelectrodes in the tubule lumen to determine the tubule length constant, the transepithelial resistance and the core resistances in the main secretory segment of the anterior Malpighian tubule of *Drosophila melanogaster* Meigen 1830. Intact pairs of anterior Malpighian tubules still attached to a small piece of gut are isolated in Ringer's solution and transferred to rest on the bottom of a perfusion bath (see Fig. 1). One microelectrode injects current into the tubule lumen of the main segment and two additional microelectrodes in the tubule lumen measure the transepithelial voltage deflections at different sites downstream. The data are then analyzed on the basis of the infinite-length cable model to yield specific and effective transepithelial and core resistances. The use of only two microelectrodes in the tubule lumen, one to inject current and the other to record voltage, yields relative resistances that are useful in qualitative before and after comparisons in a single tubule.

The usefulness of cable analysis in renal and Malpighian tubules is manifold. Cable analysis yields measures of the transepithelial electrical resistance that spans the range from leaky to tight epithelia. Leaky epithelia usually transport large volumes of fluid in isosmotic proportions, whereas tight epithelia are capable of separating solute from water, thereby forming either dilute or concentrated fluids on one side of the epithelium. Thus, cable analysis gives first clues about the general transport properties of the tubule. Supplemented with ion substitution in the bathing media, cable analysis yields measures of ionic permselectivity, and together with measurements of the intracellular voltages, cable analysis reveals the electromotive forces and resistances of basolateral and apical cell membranes. In brief, cable analysis is the necessary electrical experimental method for unravelling the mechanism and regulation of transepithelial electrolyte transport in tubular epithelia. In the present study, cable analysis has revealed a moderately tight epithelium in the main segment of the anterior Malpighian tubule of *D. melanogaster* and yielded an electrical model of transepithelial electrolyte secretion that is remarkably similar to the model of electrolyte secretion in distal tubules of *Aedes aegypti* when both tubules are studied under similar experimental conditions.

Department of Biology/Chemistry, Division of Animal Physiology, University of Osnabrück, Barbarastrasse 11, Osnabrück 49076, Germany.

\*Author for correspondence (kwb1@cornell.edu)

 K.W.B., 0000-0003-3652-2102

Received 10 February 2019; Accepted 25 April 2019

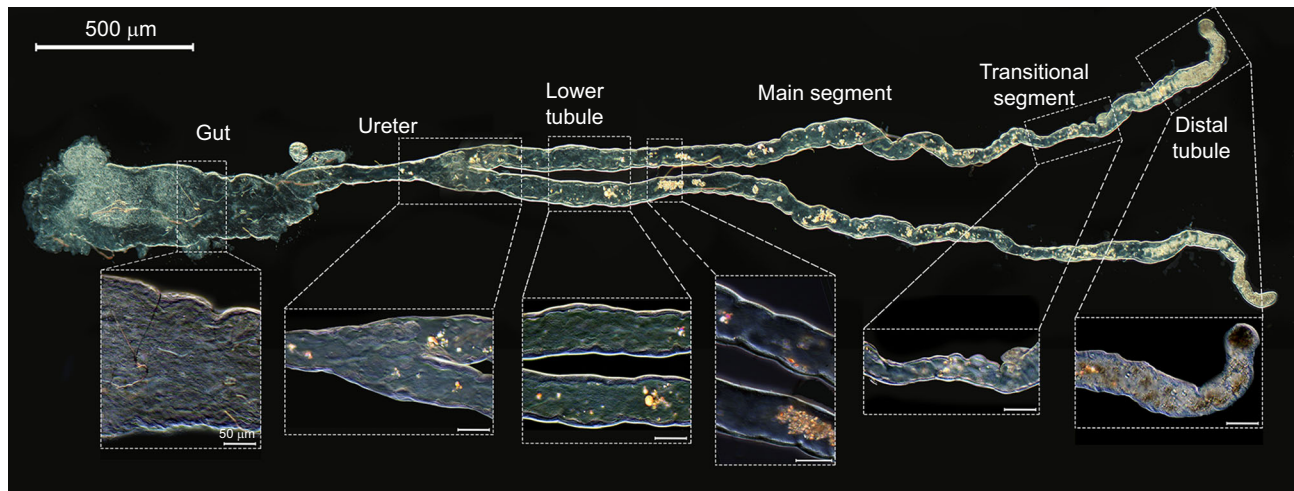


**Fig. 1. Pair of anterior Malpighian tubules of *Drosophila melanogaster* secreting fluid *in vitro*.** The distal tubule secretes xanthines, uric acid and Ca oxalates, which precipitate (flocculent material) in the tubule lumen. The transport function of the transitional segment is unknown. The main segment secretes an isosmotic fluid; however, the concentrations of secreted  $K^+$  and  $Na^+$  can vary widely depending on the peritubular  $K^+$  and  $Na^+$  concentrations with  $Cl^-$  as the preferred counter-ion. The lower tubule and the ureter may reabsorb solute and water. Peristaltic contractions of the ureter propel secreted fluid into the gut; the contractions can also be observed to move secreted fluid back and forth in the upper tubule. The upper tubule (distal, transitional and main segments) consists of ~80% principal cells and 20% stellate cells, whereas the lower tubule and the ureter do not have stellate cells (Denholm et al., 2003). Note the differences in lumen diameter along the length of the tubule. The scale bars in the insets are 50  $\mu m$ . Contractions of the ureter and the flow of tubular fluid were indicated by the movement of flocculent material in the tubule lumen.

## MATERIALS AND METHODS

### *Drosophila melanogaster*

We considered *white*<sup>1118</sup> (RRID:BDSC 5905) as the wild type. The flies were reared under standard conditions at 22°C on cornmeal agar and a 12 h:12 h light:dark light cycle. Malpighian tubules of *D. melanogaster* are formed during the first 21 h of embryogenesis at 25°C, i.e. before the hatch of the first instar larva. Thereafter, the tubules are not rebuilt during metamorphosis and remain almost unmodified to the adult stage (Denholm et al., 2003; Singh et al., 2007; Sozen et al., 1997). The development of the tubule stops as the number of cells in the upper tubule (initial, transitional and main segments of the tubule) has reached approximately 150 cells (Singh et al., 2007). Of these, 80% are principal cells with ectodermal origin and 20% are stellate cells with mesodermal origin (Jung et al., 2005; Pugacheva and Mamont, 2003; Singh et al., 2007; Sozen et al., 1997).

Adult female flies at least 5 days old were cold-anesthetized on ice. Pairs of anterior Malpighian tubules were isolated with the cold-anesthetized fly submerged in Ringer's solution as shown in the video produced in the laboratory of Rodan (Schellinger and Rodan, 2015). The main segment of the anterior tubule, which secretes most of the fluid arriving in the gut (Dow et al., 1994), was the focus of the present study.

### Ringer's solutions

The basic Ringer's solution (BRS) contained (in mmol l<sup>-1</sup>): 117.5 NaCl, 20 KCl, 2 CaCl<sub>2</sub>, 8.5 MgCl<sub>2</sub>, 10.2 NaHCO<sub>3</sub>, 15 Hepes, 4.3 NaH<sub>2</sub>PO<sub>4</sub> and 20 glucose. For measurements of transepithelial  $Cl^-$  diffusion potentials, the  $Cl^-$  concentration in BRS was reduced 10-fold, and included (in mmol l<sup>-1</sup>): 117.5 Na-gluconate, 20 K-gluconate, 2 CaCl<sub>2</sub>, 5.95 MgCl<sub>2</sub>, 3.83 MgSO<sub>4</sub>, 10.2 NaHCO<sub>3</sub>, 15 Hepes, 4.3 NaH<sub>2</sub>PO<sub>4</sub> and 20 glucose. The pH was adjusted to 7.0. The average  $[H^+]$  of all solutions was  $(9.6 \pm 0.07) \times 10^{-8}$  mol l<sup>-1</sup> ( $n=50$ ), pH 7.02. The osmotic pressures of the Ringer's solutions containing 100%  $Cl^-$  and 10%  $Cl^-$  solution were, respectively,  $335.6 \pm 1.2$  ( $n=43$ ) and  $332.3 \pm 1.3$  mOsm kg<sup>-1</sup> ( $n=6$ ) H<sub>2</sub>O. Drosokinin (JPT Peptides, Berlin, Germany) was used at a concentration of 1  $\mu$ mol l<sup>-1</sup>. To estimate the epithelial shunt resistance,  $R_{sh}$ , BRS was initially

exchanged with BRS containing 2,4-dinitrophenol (DNP), KCN and NaN<sub>3</sub> (each 1 mmol l<sup>-1</sup>). However, this inhibitory cocktail of ATP synthesis (and transcellular active transport) proved insufficient for estimates of  $R_{sh}$  owing to the high  $K^+$  conductance of basolateral membranes. For this reason, a low- $K^+$  phosphate-free BRS containing 2 mmol l<sup>-1</sup>  $K^+$ , 5 mmol l<sup>-1</sup> BaCl<sub>2</sub> and the above inhibitors of ATP synthesis was used to raise the transcellular resistance to such a degree that measures of the transepithelial resistance approached the resistance of the transepithelial shunt. The specific resistance of BRS was  $59.2 \pm 0.2 \Omega cm$  ( $n=20$ ) measured with the WTW Multimeter 3430 and the TetraCon 925 conductivity probe (Xylem Analytics, Weilheim, Germany).

Although fluid secretion rates are highest in a 1:1 mixture of BRS and Schneider's medium, *D. melanogaster* Malpighian tubules are rather insensitive to the choice of saline (Dow et al., 1994). Because the use of Schneider's medium complicated the studies of  $Cl^-$  diffusion potentials, it was omitted in the present study.

### Isolation of anterior tubules

Stable microelectrode impalements of epithelial cells and the tubule lumen required good immobilization of the Malpighian tubule in the perfusion bath. Glass cover slips were coated in three or more drying cycles with three short puffs of 0.1 mmol l<sup>-1</sup> poly-lysine (JPT Peptides Technologies GmbH, Berlin, Germany) delivered from a vaporizer and stored at 4°C. On the day of the experiment, 50  $\mu$ l of BRS was deposited on the poly-lysine-coated cover slip to receive a pair of anterior Malpighian tubules still attached to a small piece of gut. Although the tubules stick immediately here and there to the glass, they can still be straightened out by handling the piece of gut (tubules and ureter were never handled with forceps). As shown in Fig. 1, slight stretching of the tubules forms a straight line of the main segment, which facilitates the impalement with a microelectrode approaching a principal cell or the tubule lumen at an angle of 45 deg or less in line with the tubule. The bath volume was brought up to 150  $\mu$ l or 3 ml depending on the need to conserve reagent. Inflow and outflow lines allowed the change of the perfusion bath. The tubules were viewed under a Leica Stereoscope

MZ95 at magnification ranging from 16× to 150×. The distances between microelectrode tips in the tubule lumen were measured with an ocular micrometer.

### Electrophysiology

Microelectrodes were pulled with a Sutter P-97 Flaming/Brown microelectrode puller (Sutter Instruments, Novato, CA, USA) and filled with 3 mol l<sup>-1</sup> KCl. The electrical resistance for both current-injection and voltage electrodes was on average 48.9±0.9 MΩ ( $n=264$ ). After each pull, the microelectrode with the lower resistance was used as the current/voltage electrode. For the measurement of voltage, the preamplifiers HS-2A Headstage Gain x1LU and HS-2A Headstage Gain x1MGU (Axon Instruments, Molecular Devices, San Jose, CA, USA) were used. The latter preamplifier was also used to pass current for the measurement of resistance. Ag/AgCl bridges in the microelectrodes and a 4% BRS agar bridge in the perfusion bath completed the measuring circuits. When both current and voltage electrodes were lodged in a principal cell (or in the lumen), the basolateral membrane resistance  $R_{bl}$  or the transepithelial resistance  $R_t$ , respectively, were measured in six 200 ms voltage clamp steps of 5 mV bracketing the basolateral membrane voltage  $V_{bl}$  or the transepithelial  $V_t$ , respectively. The current–voltage plots (I–V plots) were usually linear in both measurements of  $R_{bl}$  and  $R_t$ . A GeneClamp 500B along with the Digidata 1322A were used to record electrophysiological data (Molecular Devices). To monitor the quality of microelectrode impalements, voltages were recorded continuously at a frequency of 10<sup>7</sup> Hz except for the brief periods of I–V plots, during which the voltage clamp was set at a gain of 1 K and a stability of 200 μs.

### The Malpighian tubule modelled as an infinite electrical cable

The measurement of the transepithelial resistance in a tubular epithelium requires cable analysis. The specific cable equations depend on the experimental condition. When the two ends of the tubule can be electrically isolated from the bathing medium, as in isolated tubules perfused by the method of Burg et al. (1966), the cable length is defined and cable analysis yields direct measurements of the length constant and the transepithelial and core resistances in renal tubules (Helman, 1972) and Malpighian

tubules (Pannabecker et al., 1993; Williams and Beyenbach, 1984). When the tubule ends are not electrically isolated, as in studies of renal tubules *in vivo* or in isolated Malpighian tubules *in vitro* as in the present study, the tubule is considered a cable of infinite length (Boulpaep and Giebisch, 1978; Frömter, 1986). The infinite cable model requires that three microelectrodes are placed in the tubule lumen for the measurement of the tubule length constant and the transepithelial and core resistances (Fig. 2).

### Measurement of specific resistances

Fig. 2 illustrates the Malpighian tubule modelled as an electrical cable consisting of a series of (1) core resistances  $r_c$ , (2) transepithelial resistances  $r_t$  in parallel to transepithelial capacitances  $c_t$  and (3) resistances of the peritubular medium  $r_p$  (bath). Because the core resistance (fluid in the tubule lumen) is much greater than the bath resistance, the latter can be neglected in the analysis of the cable. For the measurement of the specific transepithelial resistance ( $sR_t$ ), current is injected into the tubule lumen via the current/voltage electrode  $E_0$  to yield the voltage deflections  $\Delta V_{t1}$  and  $\Delta V_{t2}$ . Because the distance  $d_2$  between electrodes  $E_1$  and  $E_2$  can be measured through the microscope, Eqn 1 yields the length constant  $\lambda$  of the tubule, namely the distance in cm from the current injection site at which  $\Delta V_t$  has decayed to 37%:

$$\frac{\Delta V_{t2}}{\Delta V_{t1}} = e^{-d_2/\lambda}. \quad (1)$$

Knowledge of the length constant and the distance  $d_1$  allows determination of  $\Delta V_0$  at the site of current injection (Eqn 2):

$$\Delta V_{t0} = \frac{\Delta V_{t1}}{e^{-d_1/\lambda}}. \quad (2)$$

Because the injected current ( $\Delta I_0$ ) is known and controlled by the GeneClamp, the ratio of  $\Delta V_{t0}$  and  $\Delta I_0$  yields the input resistance,  $R_{input}$  (Eqn 3):

$$R_{input} = \frac{\Delta V_0}{\Delta I_0}. \quad (3)$$

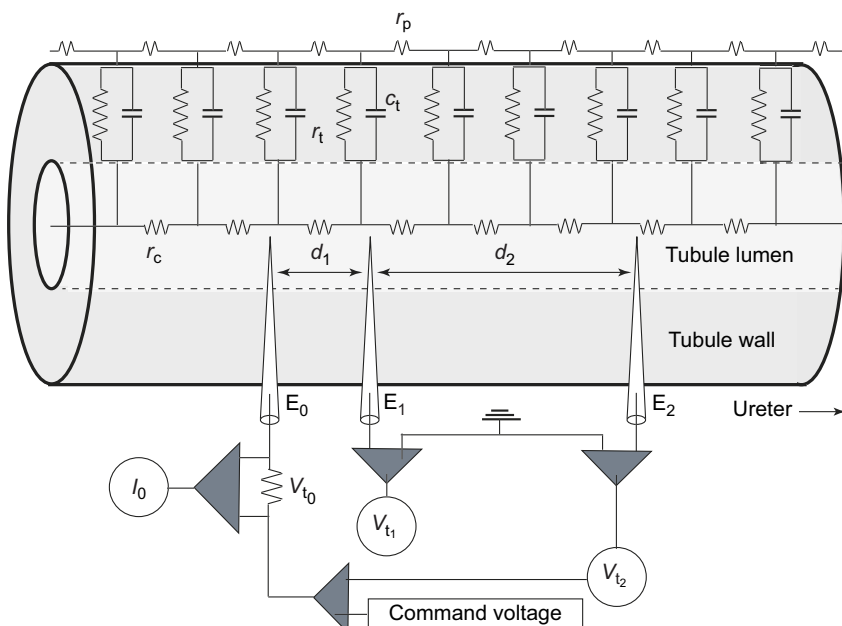


**Fig. 2. The Malpighian tubule of *D. melanogaster* modelled as an infinite electrical cable.** The cable consists of a conductive, central luminal core (secreted fluid) and a less conductive, 'insulating' single layer of epithelial cells (tubule wall). The isolated Malpighian tubule attached to the ureter and a small piece of the intestine is placed in a perfusion bath containing basic Ringer's solution, as in Fig. 1. Current  $I_0$  is injected into the tubule lumen of the main segment via microelectrode  $E_0$  with respect to ground in the bath, and the transepithelial voltage deflections are recorded downstream at  $d_1$  and  $d_2$  for the determination of the cable parameters.  $V$ , voltage;  $I$ , current;  $E$ , microelectrode;  $r_t$ , series transepithelial resistance;  $c_t$ , series transepithelial capacitance;  $r_p$ , series peritubular bath resistance;  $r_c$ , series resistance of tubule lumen (core);  $d$ , distance.



The specific transepithelial resistance  $sR_t$  normalized to luminal surface area ( $\Omega \text{ cm}^2$ ) depends on four variables: the length constant ( $\lambda$ ),  $R_{\text{input}}$ , the radius of the tubule lumen ( $r_e$ ) and the resistivity of the luminal fluid ( $\rho$ ). However, any combination of only three variables yields  $sR_t$  (Eqn 4) (Boulpaep and Giebisch, 1978). Accordingly, there are four expressions of the equation for  $sR_t$ :

$$sR_t = \frac{2\rho\lambda^2}{r_e} = \sqrt{8\pi\rho\lambda^3R_{\text{input}}} = 4\pi r_e\lambda R_{\text{input}} = \frac{8\pi^2r_e^3R_{\text{input}}^2}{\rho}, \quad (4)$$

where  $r_e$  is the electrical radius of the tubule lumen. Because the optical radius of the tubule lumen measured through the microscope varies considerably with length along the tubule (see Fig. 1),  $sR_t$  was determined in the present study with known values  $\lambda$ ,  $R_{\text{input}}$ , and  $\rho$ , the resistivity of secreted fluid in the tubule lumen; i.e. the second equivalence of Eqn 4 does not require knowledge of the lumen radius. The resistivity of secreted fluid in the tubule lumen was assumed to be similar to that of the peritubular Ringer's solution in view of (1) the secretion of fluid isosmotic to the peritubular Ringer's bath, and (2) the largely electrolyte composition of both peritubular and luminal fluids.

Rearranging Eqn 4 yields the electrical radius of the tubule lumen  $r_e$  (Eqn 5):

$$r_e = \sqrt{\frac{\rho\lambda}{2\pi R_{\text{input}}}}. \quad (5)$$

Eqn 6 relates the length constant to the specific transepithelial resistance  $sR_t$  and the specific core resistance  $sR_c$ , the resistance of the tubule lumen:

$$\lambda = \sqrt{\frac{r_e sR_t}{2sR_c}}. \quad (6)$$

Thus, the greater the lumen radius  $r_e$  and the specific transepithelial resistance, the greater the length constant and the smaller the loss of current injected into the tubule lumen. Rearrangement of Eqn 6 yields the specific core resistance  $sR_c$ :

$$sR_c = \frac{r_e sR_t}{2\lambda^2}. \quad (7)$$

### Measurement of effective resistances

Specific resistances (Eqn 4) are normalized to the area of luminal surface. Effective resistances are normalized to tubule length. Eqns 8 and 9 show, respectively, the conversions of transepithelial and core specific resistances  $sR$  to effective resistances  $eR$ :

$$eR_t = \frac{sR_t}{2\pi r_e}, \quad (8)$$

$$eR_c = \frac{sR_c}{\pi(r_e)^2}. \quad (9)$$

For effective resistances, the length constant of the tubule is:

$$\lambda = \sqrt{\frac{eR_t}{eR_c}}, \quad (10)$$

and the electrical radius of the tubule lumen is:

$$r_e = \sqrt{\frac{\rho}{\pi(eR_c)}}. \quad (11)$$

### Relative resistance

The use of only two microelectrodes in the tubule lumen yields the relative transepithelial conductance  $g_t$ , as the ratio of  $I_o$  and  $V_{t2}$ , or its inverse, the relative transepithelial resistance  $rR_t$  (Fig. 2). The relative transepithelial resistance decreases with increasing distance between current and voltage electrodes as epithelial mass between the two electrodes increases. For this reason, measures of  $rR_t$  are relative and useful only in before/after comparisons in the same tubule (paired comparisons using each tubule as its own control).

Non-linear or distorted I–V plots resulted when the tip of one electrode is not free in the tubule lumen or in the cell as in touching a membrane. Currents as high as 300 nA were injected into the tubule lumen without ill effects on the tubule.

### Measurement of the fractional resistance of the basolateral membrane of principal cells

The fractional resistance of the basolateral membrane  $fR_{bl}$  is defined as the ratio  $\Delta V_{bl}/\Delta V_t$  consequent to the passage of transepithelial current (Eqn 12).

$$fR_{bl} = \frac{\Delta V_{bl}}{\Delta V_t} = \frac{\Delta V_{bl}}{\Delta V_{bl} + \Delta V_a} = \frac{R_{bl}}{R_{bl} + R_a}, \quad (12)$$

where  $V$  is voltage,  $R$  is resistance and the subscripts bl and a denote the basolateral and apical membrane, respectively. In the typical measurement of  $fR_{bl}$ , the current electrode  $E_0$  and the voltage electrode  $E_2$  were lodged in the tubule lumen, and the voltage electrode  $E_1$  was in the cytoplasm of a principal cell (Fig. 2). The I–V plot yielded the voltage deflection across the basolateral membrane of the impaled principal cell ( $\Delta E_1 = \Delta V_{bl}$ ). Electrode  $E_1$  was subsequently advanced across apical membrane into the tubule lumen. With all three microelectrodes located in the tubule lumen, the transepithelial I/V plot yielded  $\lambda$  and consequently  $\Delta V_t$  at the site of the previously impaled principal cell for the determination  $fR_{bl}$  (Eqn 12).

### Statistical analysis

Significant differences were evaluated using the Student's *t*-test for either unpaired or paired samples.

## RESULTS

### Studies with three microelectrodes: cable analysis

Studies with three microelectrodes yield resistances normalized to luminal surface area or tubule length for comparisons with Malpighian tubules from other species and other epithelia. The tubule lumen of Malpighian tubules is easily reached by passing the microelectrode through thin stellate cells ( $<5 \mu\text{m}$ ). Passing a microelectrode through principal cells ( $>15 \mu\text{m}$ ) usually yields the basolateral membrane voltage before reaching the tubule lumen (as in Fig. 5). Under control conditions when the tubules were bathed in BRS, the transepithelial voltage was  $31.6 \pm 4.0 \text{ mV}$ , the basolateral membrane voltage of principal cells was  $-39.3 \pm 3.8 \text{ mV}$ , and the apical membrane voltage was  $70.9 \pm 4.0 \text{ mV}$  in 11 main segments of the anterior Malpighian tubule studied in Table 1.

### Estimate of the shunt resistance

According to the Ussing–Windhager conception of transepithelial transport, active and passive transport pathways are parallel across the epithelium (see Fig. 4A). The passive transport pathway is considered the shunt. In initial estimates of the shunt resistance, the cocktail of DNP,  $\text{NaN}_3$  and KCN was added to the peritubular bath to inhibit ATP synthesis and hence active transcellular transport.

**Table 1. Effect of inhibiting transcellular cation transport through principal cells on the cable parameters of the main segment of the anterior tubule of *Drosophila melanogaster***

		Control	Metabolic inhibition, low K <sup>+</sup> BRS, Ba <sup>2+</sup>	P
Normalization to luminal surface area	Tubule length constant, $\lambda$	540.0±87.8 $\mu\text{m}$	772.4±102.1 $\mu\text{m}$	<0.0491
	Electrical radius of the tubule lumen, $r_e$	21.0±2.6 $\mu\text{m}$	21.3±2.6 $\mu\text{m}$	n.s.
	Specific transepithelial resistance, $sR_t$	229.3±4.4 $\Omega \text{ cm}^2$	357.3±64.7 $\Omega \text{ cm}^2$	<0.0022
Normalization to tubule length	Specific core resistance, $sR_c$	55.8±5.0 $\Omega \text{ cm}$	63.5±3.4 $\Omega \text{ cm}$	n.s.
	Effective transepithelial resistance $eR_t$	17.1±2.4 k $\Omega \text{ cm}$	26.9±4.0 k $\Omega \text{ cm}$	<0.0004
	Effective core resistance $eR_c$	5.5±1.3 M $\Omega \text{ cm}^{-1}$	6.7±1.6 M $\Omega \text{ cm}^{-1}$	n.s.

Data are from 11 Malpighian tubules; each tubule is used as its own control. Control, in the presence of BRS in the bath; metabolic inhibition, in the presence of low K<sup>+</sup> BRS (2 mmol l<sup>-1</sup> K<sup>+</sup>), 5 mmol l<sup>-1</sup> Ba<sup>2+</sup> plus DNP, NaN<sub>3</sub> and KCN (1 mmol l<sup>-1</sup> each). The transepithelial resistance approximates the shunt resistance after metabolic inhibition in low K<sup>+</sup> BRS containing Ba<sup>2+</sup>.

The inhibition was expected to increase the transcellular resistance to such a degree that measures of the transepithelial resistance approach the resistance of the shunt as in *A. aegypti* Malpighian tubules (Pannabecker et al., 1992). Not so in *D. melanogaster* Malpighian tubules: the inhibitor cocktail failed to significantly increase the effective transepithelial resistance (control, 14.2 ±2.0 k $\Omega \text{ cm}$ ; cocktail 16.1±3.0 k $\Omega \text{ cm}$ ;  $P<0.34$ , 13 anterior tubules). However, the inhibitory cocktail of ATP synthesis significantly brought all voltages towards zero with two kinetics of voltage depolarization (Fig. 3A). The first fast depolarization (phase 1, Fig. 3A) took off as soon as the cocktail was added to the peritubular medium and lasted about the time it took to change the bath, ~25 s. In phase 1,  $V_a$  depolarized from 80 to 24 mV (lumen-positive),  $V_t$  depolarized from 33 mV and reversed polarity to -12 mV, and  $V_{bl}$  depolarized from -47 to -38 mV. Thereafter, in phase 2 of slow depolarization, voltages gradually depolarized and converged at values near 0 mV in the time of 196 s (Fig. 3A).

To elicit a sharp drop of all voltages together with a sharp increase in the transepithelial resistance, it was necessary to reduce the K<sup>+</sup> conductance of basolateral membranes in addition to the inhibition of ATP synthesis. As shown in Fig. 3B, the inhibitory cocktail together with 5 mmol l<sup>-1</sup> Ba<sup>2+</sup> in low K<sup>+</sup> (2 mmol l<sup>-1</sup>) BRS promptly depolarized all voltages in the time it took to replace the peritubular bath. Moreover, the K<sup>+</sup> channel blocker Ba<sup>2+</sup> in low K<sup>+</sup> peritubular Ringer's solution obliterated phase 2 of depolarization as well as the reversal of the transepithelial voltage to lumen-negative values. In subsequent studies of 11 main segment of anterior Malpighian tubules, the combined effects of metabolic inhibition and reduced K<sup>+</sup> conductance significantly increased the tubule length constant from 540.0 to 772.4  $\mu\text{m}$  and significantly increased the effective transepithelial resistance  $eR_t$  from 17.1 to 26.9 k $\Omega \text{ cm}$  (Table 1). The lack of a significant effect on the effective core resistance  $eR_c$  and the electrical radius of the tubule lumen point to the successful inhibition of, specifically, the transcellular active transport pathway (Table 1).

#### Electrical equivalent model of transepithelial electrolyte secretion in the main segment of the anterior Malpighian tubule of *D. melanogaster*

The transepithelial secretion (or absorption) of electrolytes such as Na<sup>+</sup>, K<sup>+</sup> and Cl<sup>-</sup> carries current and generates voltages. Accordingly, the transepithelial secretion of electrolytes in the main segment of the anterior Malpighian tubule can be modelled with an electrical circuit consisting of two transepithelial routes for current flow: an active transport pathway leading through cells where active transport finds ATP, parallel to a passive transport pathway, the shunt that does not require ATP (Fig. 4A). In general, Na<sup>+</sup> and K<sup>+</sup> are actively transported through principal cells, and Cl<sup>-</sup> is passively transported through stellate cells and/or the paracellular pathway (Beyenbach and Piermarini, 2011; O'Donnell et al., 1996;

Pannabecker et al., 1993). The analysis of electrical equivalent circuits is useful in that it reveals (1) the driving forces for electrolyte secretion across the basolateral and apical membranes, and (2) the electrical resistances of all three barriers: basolateral membrane, apical membrane and shunt. Knowledge of these variables is useful for further dissection of transport pathways. For example, the analysis of an electrical equivalent circuit of Malpighian tubules in *A. aegypti* has shown *inter alia* that (1) the conductance of the basolateral membrane of principal cells is

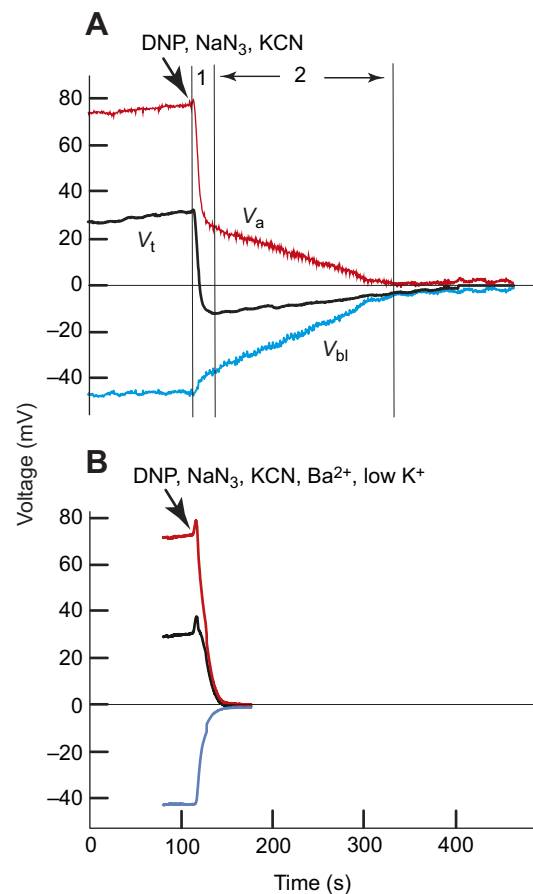


**Fig. 3. Inhibition of voltage generation in the main segment of the anterior Malpighian tubule of *D. melanogaster*.** (A) Fast (1) and slow (2) kinetics of voltage depolarization upon adding DNP, NaN<sub>3</sub> and KCN (1 mmol l<sup>-1</sup> each) to the peritubular bath (arrow). (B) Loss of the slow phase of depolarization when the peritubular medium was replaced with basic Ringer's solution containing 2 mmol l<sup>-1</sup> K<sup>+</sup> and 5 mmol l<sup>-1</sup> Ba<sup>2+</sup> as well as the inhibitory cocktail of ATP synthesis.  $V_a$ , apical membrane voltage of a principal cell;  $V_{bl}$ , basolateral membrane voltage;  $V_t$ , transepithelial voltage.

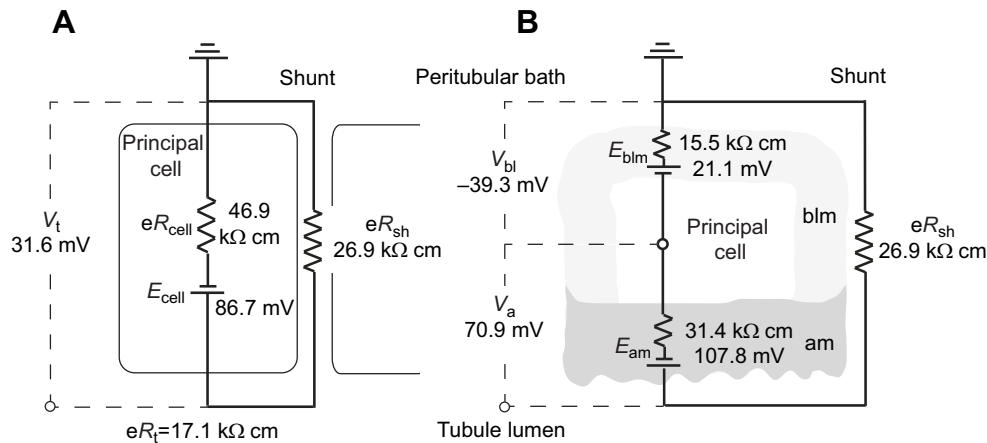


**Fig. 4. Models of transepithelial electrolyte transport and secretion in the main segment of the anterior Malpighian tubule of *D. melanogaster*.** (A) The Ussing–Windhager model of transepithelial electrolyte transport. Parallel transepithelial active and passive (shunt) transport pathways (Ussing and Windhager, 1964). The active transport pathway leads through cells where the electromotive force ( $E$ ) for transport is generated; the passive transport pathway, i.e. the shunt, may pass through cells or between cells. Thus, positive  $\text{Na}^+$  and  $\text{K}^+$  current passes through principal cells into the tubule lumen; positive current returns to the peritubular bath via  $\text{Cl}^-$  secretion through the shunt. (B) Distributed circuit model of transepithelial electrolyte secretion. Electromotive forces and resistances of the basolateral and apical membrane of principal cells of the main segment. Electrical resistances are expressed in terms of tubule length ( $eR$ ).  $V$ , voltage; am, apical membrane; blm, basolateral membrane; sh, shunt.

dominated by  $\text{K}^+$ , (2) the conductance of the apical membrane is dominated by the V-type ATPase, and (3) the diuretic hormone leucokinin increases the  $\text{Cl}^-$  conductance of the shunt pathway (Beyenbach, 2012; Beyenbach and Masia, 2002; Beyenbach et al., 2000b; Beyenbach and Wieczorek, 2006; Pannabecker et al., 1993).

In the case of the electrical equivalent circuit of transepithelial electrolyte transport in anterior Malpighian tubules of *D. melanogaster*, the estimate of the shunt resistance allows estimates of the electromotive forces and resistances of the transcellular pathway under control conditions (Fig. 4). Effective rather than specific resistances are used from here on for comparison with Malpighian tubules of *A. aegypti* (Pannabecker et al., 1992). However, the purpose

of this paper is not this comparison but to introduce a new experimental method: the measurement of resistance in tubular epithelia as small as Malpighian tubules of *D. melanogaster* using cable analysis and conventional microelectrodes rather than the method of *in vitro* microperfusion of tubules.

According to the minimal electrical model of transepithelial electrolyte secretion (Fig. 4A), the open-circuit current  $I_{oc}$  is:

$$I_{oc} = \frac{E_{cell}}{eR_{cell} + eR_{sh}} = \frac{V_t}{eR_{sh}}, \quad (13)$$

where  $E_{cell}$  and  $eR_{cell}$  are the electromotive force and the effective resistance of the transcellular transport pathway, respectively, and  $eR_{sh}$  is the effective resistance of the shunt (Fig. 4A,B). Accordingly:

$$V_t = \frac{E_{cell} eR_{sh}}{eR_{cell} + eR_{sh}}. \quad (14)$$

The effective transepithelial resistance  $eR_t$  is:

$$eR_t = \frac{eR_{cell} eR_{sh}}{eR_{cell} + eR_{sh}}. \quad (15)$$

Because  $eR_t$  is 17.1  $\text{k}\Omega \text{ cm}$  and  $eR_{sh}$  is 26.9  $\text{k}\Omega \text{ cm}$  (Table 1), the effective transcellular resistance  $eR_{cell}$  is 46.9  $\text{k}\Omega \text{ cm}$  (Fig. 4A).

The ratio of the transepithelial voltage and transepithelial resistance is the short-circuit current  $I_{sc}$ , i.e. the maximum current under any condition when transcellular current is not slowed down by the resistance of the epithelial shunt:

$$I_{sc} = \frac{V_t}{eR_t} = \frac{E_{cell}}{eR_c}. \quad (16)$$

Because  $V_t$  is 31.6 mV and  $eR_t$  is  $17.1 \pm 2.4 \text{ k}\Omega \text{ cm}$  (Table 1),  $I_{sc}$  is  $1.85 \mu\text{A cm}^{-1}$  and  $E_{cell}$  is 86.7 mV for a transcellular resistance of 46.9  $\text{k}\Omega \text{ cm}$  (Fig. 4A). The fractional resistance of the basolateral membrane of principal cells was  $0.33 \pm 0.05$  in nine main segments of the anterior tubule (Eqn 12). Accordingly, the effective resistance of the basolateral membrane  $eR_{bl}$  is 15.5  $\text{k}\Omega \text{ cm}$ , and the effective apical membrane resistance  $eR_a$  is 31.4  $\text{k}\Omega \text{ cm}$  (Fig. 4B). Knowledge of these resistances yields the voltage drops across

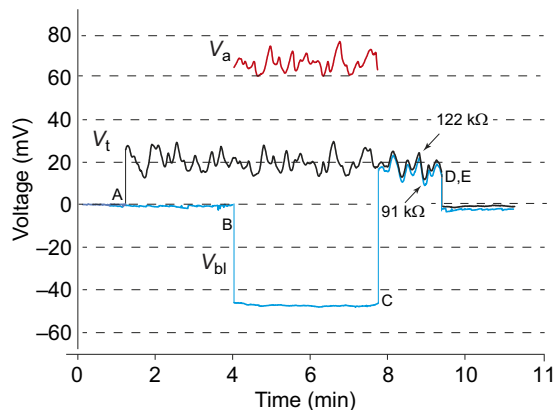


**Fig. 5. Spontaneous oscillations of the transepithelial voltage and resistance in the main segment of an anterior Malpighian tubule of *D. melanogaster*.** (A) Impalement of the tubule lumen with the current/voltage microelectrode to measure the transepithelial voltage  $V_t$ . (B) Impalement of a principal cell with the voltage microelectrode to measure the basolateral membrane voltage  $V_{bl}$ . (C) Passing the voltage microelectrode through the apical membrane into the tubule lumen to record  $V_t$ . (D,E) Withdrawal of both microelectrodes to the peritubular bath (ground). The apical membrane voltage  $V_a$  is the difference between  $V_t$  and  $V_{bl}$ . Relative resistance (not normalized to tubule length) was measured in this study with two microelectrodes. Note that the effective transepithelial resistance ( $eR_t$ ) and  $V_t$  cycle in parallel:  $eR_t$  increases as  $V_t$  increases.

$eR_{bl}$  and  $eR_a$  under open-circuit conditions as well as the electromotive force  $E$  of the basolateral and apical membrane when the tubule secretes electrolytes and fluid.

According to Eqn 13, the open-circuit current  $I_{oc}$  is  $1.17 \mu A cm^{-1}$  (Fig. 4A). Hence, the voltage drop across  $eR_{bl}$  is 18.2 mV (cell negative) and  $E$  of the basolateral membrane ( $E_{bl}$ ) is cell-negative 21.1 mV (Fig. 4B). The voltage drop across  $eR_a$  is 36.9 mV and  $E$  of the apical membrane ( $E_a$ ) is also cell-negative 107.8 mV (Fig. 4B).

### Studies with two microelectrodes

Studies with two microelectrodes, one to inject current and the other to record voltage, yield relative resistances that are useful for comparing before/after effects using each tubule as its own control. As relative resistances are not normalized to tubule length or area, they should not be used for comparison with other tubules or epithelia.

### The transepithelial voltage profile

Fig. 5 illustrates a representative experiment using two microelectrodes. The two microelectrodes are located within 600  $\mu m$  of each other in the main segment of an anterior tubule; on average, the distance between the two electrodes was  $357.4 \pm 30.1 \mu m$  in 25 tubules. The tip of the current–voltage microelectrode has entered the tubule lumen at point A to record the lumen-positive transepithelial voltage ( $V_t$ ).  $V_t$  is usually constant with time, but oscillating voltages were observed occasionally. The tip of the other microelectrode has penetrated the basolateral membrane of a principal cell at point B to record the cell-negative basolateral membrane voltage ( $V_{bl}$ ). Significantly,  $V_{bl}$  does not oscillate but remains constant near  $-50$  mV. It follows that oscillations of  $V_t$  parallel oscillations of the apical membrane voltage ( $V_a$ ).  $V_a$  was not measured directly but was determined as the difference between  $V_t$  and  $V_{bl}$  in accordance with Kirchhoff's law. At point C, the voltage microelectrode has been advanced across the apical membrane of the impaled principal cell into the tubule lumen. Both microelectrodes now measure  $V_t$ . With both microelectrode tips lodged in the tubule lumen, the relative transepithelial resistance ( $rR_t$ ) is measured with a current–voltage plot. When  $V_t$  had hyperpolarized to 25 mV,  $rR_t$  was 122 k $\Omega$ ; when  $V_t$  had depolarized to 10 mV,  $rR_t$  was 91 k $\Omega$  (Fig. 5).

### The effect of drosokinin on transepithelial voltage and resistance

In the experiment shown in Fig. 6, the tips of both microelectrodes were lodged in the tubule lumen of the main segment of an anterior Malpighian tubule and recorded similar values of the transepithelial voltage. Shortly before adding drosokinin ( $1 \mu mol l^{-1}$ ) to the peritubular bath,  $V_t$  was 26 mV and  $rR_t$  was 109 k $\Omega$ . Upon the addition of drosokinin,  $V_t$  promptly dropped towards 0 mV; in parallel,  $rR_t$  dropped to 87 k $\Omega$ .

In paired  $t$ -tests, using each tubule as its own control, the addition of  $1 \mu mol l^{-1}$  drosokinin to the peritubular bath significantly hyperpolarized  $V_{bl}$  to  $-53.5 \pm 2.5$  mV ( $n=4$ ) ( $P<0.04$ ), significantly depolarized  $V_t$  to  $4.7 \pm 2.1$  mV ( $n=11$ ) ( $P<10^{-6}$ ), but had no significant effect on  $V_a$   $64.0 \pm 2.5$  mV ( $n=3$ ). The relative transepithelial resistance significantly decreased from  $111.5$  to  $55.0 \pm 11.8$  k $\Omega$  ( $n=25$ ) ( $P<0.02$ ).

### The $Cl^-$ dependence of the effect of drosokinin

Because the kinins – leucokinin in *A. aegypti* Malpighian tubules and drosokinin in *D. melanogaster* Malpighian tubules – are known to increase the permeability of Malpighian tubules to  $Cl^-$ , the effect of drosokinin on transepithelial  $Cl^-$  diffusion potentials was of interest (Cabrero et al., 2014; Halberg et al., 2015; Lu et al., 2011;

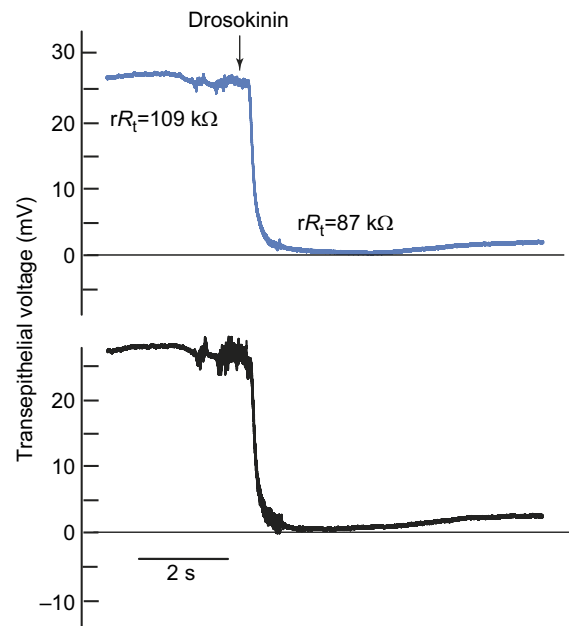


**Fig. 6. The effect of drosokinin ( $1 \mu mol l^{-1}$ ) on the transepithelial voltage and relative resistance ( $rR_t$ ) in the middle segment of an anterior Malpighian tubule of *D. melanogaster*.** The tips of both microelectrodes are located in the tubule lumen and record the transepithelial voltage. One electrode is used to pass current for measurement of the relative transepithelial resistance. Drosokinin effectively short-circuits the transepithelial voltage ( $V_t=0$  mV) and significantly lowers the relative transepithelial resistance consistent with the decrease in the transepithelial shunt resistance. Two electrode studies are suitable for before/after comparisons of the transepithelial resistance in single tubules.

Pannabecker et al., 1993; Yu and Beyenbach, 2001; Yu and Beyenbach, 2002). A representative experiment is shown in Fig. 7. In BRS containing  $158.5 mmol l^{-1} Cl^-$ ,  $V_t$  was 25 mV and the  $rR_t$  149 k $\Omega$  (Fig. 7, 9 min). The basolateral membrane voltage of a principal cell was  $-40$  mV and the apical membrane voltage was 65 mV (data not shown). The 10-fold reduction of the peritubular  $Cl^-$  concentration had negligible effects on  $V_t$  and  $rR_t$  in the absence of drosokinin (Fig. 7, 9–31 min). The addition of drosokinin ( $1 \mu mol l^{-1}$ ) to the peritubular bath had major effects on the transepithelial voltage and resistance. Drosokinin depolarized  $V_t$  from 25 to 4 mV and reduced  $rR_t$  from 161 to 49 k $\Omega$  (Fig. 7, 43 min). In the presence of drosokinin, the 10-fold reduction of the peritubular  $Cl^-$  concentration induced a large transepithelial  $Cl^-$  diffusion potential of 40 mV (Fig. 7, 67 min) and  $rR_t$  increased from 49 to 128 k $\Omega$ . After 44 min in the presence of 10% peritubular  $Cl^-$  concentration, the return to 100%  $Cl^-$  concentration in the peritubular bath returned  $V_t$  to 2 mV, consistent with the transepithelial electrical short circuit induced by drosokinin as  $rR_t$  decreased to 92 k $\Omega$  (Fig. 7, 97 min).

### DISCUSSION

Measurements of the transepithelial electrical resistance in Malpighian tubules of *D. melanogaster* have not been thought feasible because of the small size of the tubules (Blumenthal, 2001). Since the time of this assessment, *D. melanogaster* Malpighian tubules have been successfully perfused *in vitro*, which renders them suitable for measurements of the transepithelial resistance (Wu et al., 2015). The present paper presents less demanding methods using conventional microelectrodes and commercially available electronic hardware. Resistance measurements normalized to



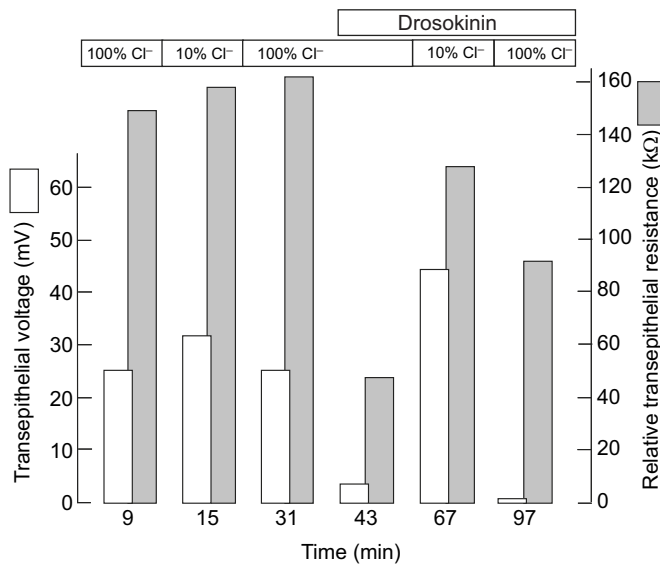


**Fig. 7. The effect of drosokinin ( $1 \mu\text{mol l}^{-1}$ ) on the transepithelial voltage and relative transepithelial resistance of the main segment of an anterior Malpighian tubule of *D. melanogaster*.** The  $\text{Cl}^-$  dependence of the drosokinin effect is demonstrated in tenfold reductions of the peritubular  $\text{Cl}^-$  concentration which hyperpolarizes the transepithelial voltage ( $V_t$ ) by 40 mV while increasing the relative transepithelial resistance ( $rR_t$ ) from 49 to 128 kΩ. Note that  $V_t$  and  $R_t$  change together as in spontaneous oscillations (Fig. 6), consistent with the shunt as the route for  $\text{Cl}^-$  secretion. Relative resistance was measured with two microelectrodes for before/after comparisons in a single tubule.

luminal surface area or tubule length require the use of three microelectrodes. The use of only two microelectrodes yields relative resistances for before/after comparisons in a single tubule.

The specific transepithelial resistance of the main segment of the anterior tubule of *D. melanogaster* is  $229.3 \Omega \text{ cm}^2$  (Table 1). By comparison,  $sR_t$  of the renal proximal tubule, a leaky epithelium, is only 6 and  $7 \Omega \text{ cm}^2$  in the rat and dog, respectively,  $30 \Omega \text{ cm}^2$  in the rabbit gall bladder,  $75 \Omega \text{ cm}^2$  in frog choroid plexus,  $100 \Omega \text{ cm}^2$  in the rabbit ileum, between 150 and  $300 \Omega \text{ cm}^2$  in the rat distal tubule,  $867 \Omega \text{ cm}^2$  in rabbit cortical collecting tubules,  $1500 \Omega \text{ cm}^2$  in the toad urinary bladder, and  $3600 \Omega \text{ cm}^2$  in the frog skin (Boulpaep and Seely, 1971; Dor'ó, 1968; Erlj, 1976; Frizzell and Schultz, 1972; Hegel et al., 1967; Helman et al., 1971; Malnic and Giebisch, 1972; Reuss and Finn, 1974; Ussing and Windhager, 1964; Wright, 1972). Accordingly, the specific transepithelial resistance of the main segment of the anterior Malpighian tubule of *D. melanogaster* falls in the range of renal distal tubules, namely moderately tight epithelia, reflecting selective barrier and transport properties

consistent with a wide quantitative and qualitative range of transepithelial transport (Beyenbach, 1993a, 2016). Resistances can also be expressed in terms of tubule length (Eqns 8 and 9). Accordingly, the specific transepithelial resistance of  $229.3 \Omega \text{ cm}^2$  is equivalent to the effective transepithelial resistance of  $17.1 \text{ k}\Omega \text{ cm}$  (Tables 1 and 2, Fig. 4).

### Validation of the cable analysis

Table 2 lists the voltages and effective resistances of the main segment of the anterior Malpighian tubule of *D. melanogaster* measured in the present study. The transepithelial voltage, 31.6 mV, measured with microelectrodes is similar to that measured in the laboratory of Rodan using the method of *in vitro* microperfusion of Malpighian tubules (Wu et al., 2015), and the basolateral membrane voltage of principal cells,  $-45.3 \text{ mV}$ , is similar to that measured in the laboratory of O'Donnell using double-barreled microelectrodes (Janowski and O'Donnell, 2004). The ratio of the transepithelial voltage and the effective shunt resistance yields the open-circuit current  $I_{oc}$  (Eqn 13), namely the intraepithelial current when tubules are secreting solutes and water into the lumen. The  $I_{oc}$  of  $1.17 \mu\text{A cm}^{-1}$  is equivalent to a transepithelial flux of  $12.1 \text{ pmol s}^{-1} \text{ cm}^{-1}$  monovalent ions. Accordingly,  $12.1 \text{ pmol}$  of cations pass per second through principal cells from bath to tubule lumen in a tubule segment 1 cm long, and  $12.1 \text{ pmol}$  of anions per second pass via the transepithelial shunt (paracellular pathway and/or stellate cells). Rates of the secretory cation flux measured in the laboratories of Dow, O'Donnell and Rodan are, on average,  $89 \text{ pmol min}^{-1}$  and stem largely from the main segment that comprises approximately 60% of the tubule length (Dow et al., 1998; Linton and O'Donnell, 1999; O'Donnell and Maddrell, 1995; Rodan et al., 2012; Wu et al., 2015). Because the average *D. melanogaster* Malpighian tubule is 2.2 mm long (Rheault and O'Donnell, 2004), the flux of  $89 \text{ pmol min}^{-1}$  for the whole tubule is equivalent to  $11.2 \text{ pmol s}^{-1} \text{ cm}^{-1}$  tubule length. The latter is in good agreement with  $12.1 \text{ pmol s}^{-1} \text{ cm}^{-1}$  measured by electrophysiological methods in the present study, and confirms (1) the cable analysis and the model of the tubule as a cable of infinite length, and (2) the largely electrogenic nature of transepithelial cation secretion.

### Estimate of the epithelial shunt resistance

According to the Ussing–Windhager conception of transepithelial NaCl transport by the frog skin,  $\text{Na}^+$  takes the active transport pathway in parallel with  $\text{Cl}^-$  through the shunt (Ussing and Windhager, 1964). The separation of transepithelial cation and anion transport applies widely to absorptive and secretory epithelia. In the case of insect Malpighian tubules in general and *D. melanogaster* Malpighian tubules in particular, the cations  $\text{Na}^+$  and  $\text{K}^+$  are secreted through principal cells, and  $\text{Cl}^-$ , the counter ion

**Table 2. Electrical variables of the main (secretory) segment of anterior tubule of *Drosophila melanogaster* and the main secretory distal (blind end) Malpighian tubule of the yellow fever mosquito, *Aedes aegypti***

	Transepithelial		Shunt Effective resistance (kΩ cm)	Basolateral membrane		Apical membrane	
	Voltage (mV)	Effective resistance (kΩ cm)		Voltage (mV)	$fR_{bl}$	Voltage (mV)	$fR_a$
<i>D. melanogaster</i>	$31.6 \pm 4.0$ (11)	$17.1 \pm 2.4$ (11)	$26.9 \pm 4.0$ (11)	$-45.3 \pm 1.0$ (54)	$0.33 \pm 0.05$ (9)	$69.4 \pm 2.0$ (52)	$0.67 \pm 0.05$ (9)
<i>A. aegypti</i>	$52.6 \pm 10.4$ (7)	$11.4 \pm 1.6$ (7)	$16.8 \pm 2.2$ (7)	$-58.0 \pm 5.2$ (7)	$0.68 \pm 0.04$ (7)	$110.6 \pm 6.3$ (7)	$0.32 \pm 0.04$ (7)
<i>P</i> -value	<0.025	<0.05	<0.05	<0.05	<0.005	<0.0005	<0.005

Note the significant difference of every variable when *D. melanogaster* and *A. aegypti* Malpighian tubules are bathed, respectively, in 20 and  $3.4 \text{ mmol l}^{-1} \text{ K}^+$  Ringer's solution. *V* and *R* are voltage and resistance, respectively, and the subscripts a, bl and sh are apical membrane, basolateral membrane and transepithelial shunt, respectively. The data for *A. aegypti* are from Pannabecker et al. (1992). Data are means  $\pm$  s.e.m. (number of tubules).  $V_t$  measured in *D. melanogaster* Malpighian tubules ( $31.6 \text{ mV}$ ) is substantially less than 50 to 60 mV measured by Blumenthal (2003). However, Blumenthal studied tubules bathed in a 1:1 mixture of basic Ringer's solution:Schneider's, which is known to increase  $V_t$ .



of  $\text{Na}^+$  and  $\text{K}^+$ , is secreted through the shunt (Beyenbach and Piernarini, 2011; O'Donnell et al., 1996). Thus, the transepithelial secretion of  $\text{Na}^+$ ,  $\text{K}^+$  and  $\text{Cl}^-$  in *D. melanogaster* Malpighian tubules can be modelled with an electrical circuit consisting of the electromotive force  $E_{\text{cell}}$  for the transcellular secretion  $\text{Na}^+$  and  $\text{K}^+$  in series with the transcellular resistance  $eR_{\text{cell}}$ , both parallel to the transepithelial shunt  $R_{\text{sh}}$  for  $\text{Cl}^-$  (Fig. 4A). An  $E_{\text{cell}}$  of 86.7 mV polarized to move positive charge ( $\text{Na}^+$ ,  $\text{K}^+$ ) into the tubule lumen is the sum of the electromotive forces of the basolateral and apical membranes for transcellular  $\text{Na}^+$  and  $\text{K}^+$  secretion (Fig. 4A). The distributed circuit reveals an electromotive force of 21.1 mV across the basolateral membrane of principal cells that reflects in part the  $\text{K}^+$  equilibrium potential across that membrane (Fig. 4B). The  $E_a$  of 107.8 mV across the apical membrane likely reflects the electromotive force of the V-type  $\text{H}^+$  ATPase located at that membrane.

In *A. aegypti* Malpighian tubules, the inhibition of ATP synthesis brings transepithelial electrolyte and fluid secretion to a halt and all voltages to zero in a matter of seconds (Beyenbach et al., 2000b; Pannabecker et al., 1992; Wu and Beyenbach, 2003). With transcellular cation secretion inhibited and  $eR_{\text{cell}}$  at a maximum, the transepithelial resistance approaches the resistance of the shunt, 16.8 k $\Omega$  cm (Table 2). This approach for estimating the shunt resistance is successful in epithelia powered largely, if not exclusively, by active transport pumps. The approach does not work in epithelia powered in addition by secondary active transport mechanisms and diffusion potentials. For example, the inhibition of ATP synthesis in the gall bladder has no effect on the transepithelial resistance, and it hyperpolarizes both basolateral and apical membrane voltages on account of ATP-sensitive  $K^+$  channels (Bello-Reuss et al., 1981). In the present study of *D. melanogaster* Malpighian tubules, the inhibition of ATP synthesis failed also to significantly increase the transepithelial resistance during the initial

phase 1 of voltage depolarization because of the large  $K^+$  conductance of the basolateral membrane (Fig. 3A). The large  $K^+$  conductance accounts for nearly 75% of the basolateral membrane voltage and the lumen-negative transepithelial voltage during phase 1 (Fig. 3A). Subsequently, in phase 2 of slow depolarization, all voltages decay gradually to zero as  $K^+$  leaks to the peritubular bath in the absence of ATP (Fig. 3A). In order to reduce the  $K^+$  conductance of the basolateral membrane, the inhibitory cocktail was fortified with the  $K^+$  channel blocker barium and the peritubular  $K^+$  concentration was reduced to  $2 \text{ mmol l}^{-1}$ . As shown in Fig. 3B, this manoeuvre brought all voltages to zero in the time it took to replace the peritubular medium. At the same time, the transcellular resistance increased to values that allowed the estimate of the effective shunt resistance,  $26.9 \text{ k}\Omega \text{ cm}$  (Fig. 4, Tables 1 and 2).

### Transepithelial voltage and resistance oscillations and the effect of kinins

Oscillations of the transepithelial voltage ( $V_t$ ) are widely observed in Malpighian tubules of insects, among them *Carausius* (Pilcher, 1970), *Locusta* (Morgan and Mordue, 1981), *Aedes* (Williams and Beyenbach, 1984) and *Drosophila* (Davies et al., 1995).  $V_t$  oscillations are also observed in the present study, which paralleled oscillations of the transepithelial resistance as in *A. aegypti* Malpighian tubules ( $R_t$ ) (Fig. 5). As  $V_t$  depolarized towards zero,  $R_t$  decreased, and as  $V_t$  hyperpolarized,  $R_t$  increased, as in *A. aegypti* Malpighian tubules, where the oscillations are dependent on the peritubular  $\text{Cl}^-$  concentration (Beyenbach et al., 2000a). In particular, as  $R_t$  decreases,  $V_t$  decreases towards the transepithelial  $\text{Cl}^-$  equilibrium potential in *A. aegypti* Malpighian tubules, revealing cyclical changes in transepithelial  $\text{Cl}^-$  conductance.

Whereas oscillations of  $V_t$  and  $R_t$  reflect transient changes in the shunt  $\text{Cl}^-$  conductance, drosokinin brings both voltage and resistance to lower constant values in *D. melanogaster* Malpighian

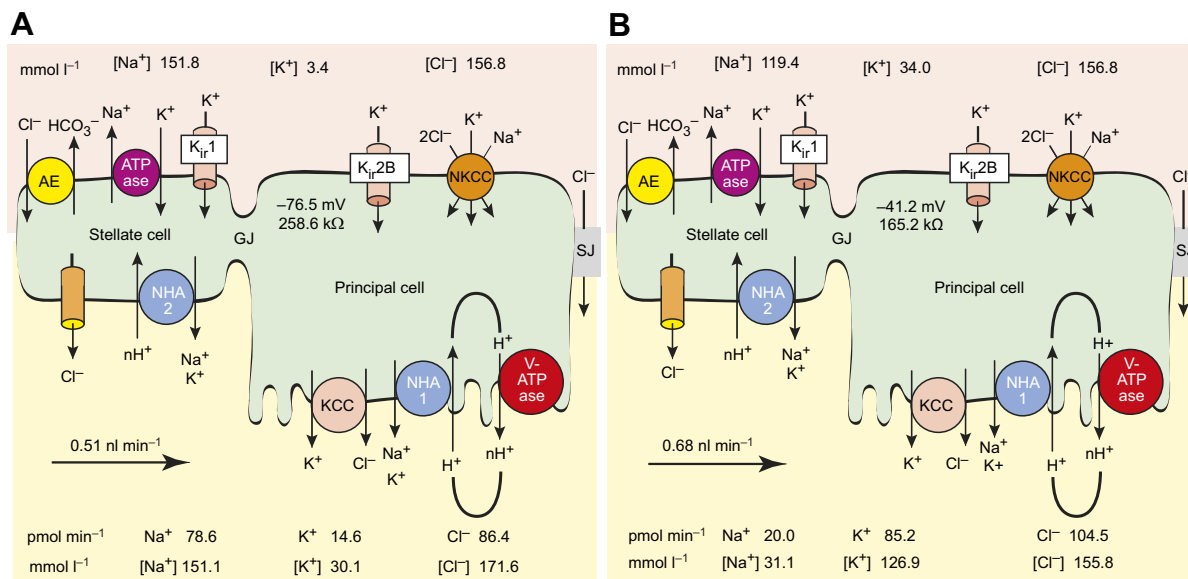


**Fig. 8. The effect of peritubular K<sup>+</sup> concentration on transepithelial electrolyte and fluid secretion in *Aedes aegypti* Malpighian tubules.** Distal segments, i.e. the blind ends of tubules were studied in the presence of 3.4 mmol l<sup>-1</sup> K<sup>+</sup> (A) and 34 mmol l<sup>-1</sup> K<sup>+</sup> (B) in the peritubular medium. The voltage and resistance of the basolateral membrane of principal cells was measured with both current and voltage electrodes located in principal cells. GJ, gap junction; SJ, septate junction; AE, anion exchanger; ATPase, Na<sup>+</sup>/K<sup>+</sup> pump; K<sub>ir</sub>, inward rectifier K<sup>+</sup> channel; NKCC, Na<sup>+</sup>/K<sup>+</sup>/2Cl<sup>-</sup> cotransporter; NHA, Na<sup>+</sup>/H<sup>+</sup> exchanger; KCC, K<sup>+</sup>/Cl<sup>-</sup> cotransporter; V-ATPase, vacuolar-type proton pump. Data are in part from Beyenbach and Masia, 2002; Hegarty et al., 1991; Hine et al., 2014; Janowski et al., 2004; O'Connor and Beyenbach, 2001; Petzel, 2000; Piermarini et al., 2015; Piermarini et al., 2010; Piermarini et al., 2011; Piermarini et al., 2013; Rheault et al., 2007; Rodan et al., 2012; Tiburcy et al., 2013; Weng et al., 2003; Weng et al., 2008; Xiang et al., 2012.

tubules, as in *A. aegypti* Malpighian tubules in the presence of leucokinin (Fig. 6) (Miyachi et al., 2011; Pannabecker et al., 1993; Schepel et al., 2010; Yu and Beyenbach, 2001). Drosokinin is the leucokinin of *D. melanogaster*. It has a single gene that encodes the longest known leucokinin with 15 amino acid residues (Radford et al., 2002). So far, only one drosokinin G protein-coupled receptor (GPCR; CG10626) has been identified in specifically stellate cells of Malpighian tubules of *Drosophila melanogaster*, *Anopheles stephensi* and *Aedes aegypti* (Lu et al., 2011; Radford et al., 2002; Radford et al., 2004). Binding to its GPCR at the basolateral membrane of stellate cells, drosokinin increases the intracellular  $[Ca^{2+}]$  in selectively stellate cells in *D. melanogaster* Malpighian tubules (Cabrero et al., 2013; Cabrero et al., 2014; O'Donnell et al., 1998; Terhzaz et al., 1999). In a comprehensive study of the mechanism of action of drosokinin, Cabrero et al. (2014) offer strong evidence for localizing the kinin-activated transepithelial  $Cl^{-}$  shunt to stellate cells of *D. melanogaster* Malpighian tubules.  $Ca^{2+}$  imaging, Ramsay fluid secretion assays, measurements of transepithelial voltage, and transgenic chloride reporter technology are consistent with the chloride channel  $CLC-a$  at the apical membrane of stellate cells as part of the kinin-activated transepithelial shunt (Cabrero et al., 2014).

### Effect of the peritubular $K^{+}$ concentration in Malpighian tubules of *D. melanogaster* and *A. aegypti*

Table 2 compares the electrophysiological variables of the main secretory segments of Malpighian tubules in two dipterans, *D. melanogaster* and *A. aegypti*, separated by 189 million years of evolution (Chen et al., 2015). Every variable is significantly different. Though time for evolution could account for the differences, they can largely be attributed to the use of different peritubular  $K^{+}$  concentrations. *Drosophila melanogaster* Malpighian tubules were bathed in  $20\text{ mmol l}^{-1} K^{+}$  and *A. aegypti* Malpighian tubules in  $3.4\text{ mmol l}^{-1} K^{+}$  Ringer's solution (Table 2). The physiological differences between *D. melanogaster* and *A. aegypti* Malpighian tubules disappear when both tubules are bathed in either low  $K^{+}$  or high  $K^{+}$  Ringer's solutions.

In the presence of the usual  $20\text{ mmol l}^{-1} K^{+}$  in the Ringer's solution, Malpighian tubules of *D. melanogaster* secrete KCl-rich fluid with a  $K^{+}$  concentration ( $180\text{ mmol l}^{-1}$ ) 9-fold higher than the concentrations of  $Na^{+}$  (Dow et al., 1994; Dow et al., 1998; Linton and O'Donnell, 1999; O'Donnell and Maddrell, 1995; Rheault and O'Donnell, 2001; Rodan et al., 2012). However, in  $K^{+}$ -free Ringer's solution, the tubules secrete a NaCl-rich fluid containing  $150\text{ mmol l}^{-1} Na^{+}$ , like *A. aegypti* Malpighian tubules (Linton and O'Donnell, 1999). What is more, in  $K^{+}$ -free Ringer's solution, cAMP stimulates fluid secretion by 48%, presumably via the stimulation of transepithelial  $Na^{+}$  secretion, as in *A. aegypti* Malpighian tubules (Beyenbach, 1993b; Beyenbach, 2003; Beyenbach and Petzel, 1987; Linton and O'Donnell, 1999; Williams and Beyenbach, 1983). The corollary is observed in *A. aegypti* Malpighian tubules.

As shown in Fig. 8A, Malpighian tubules of *A. aegypti* secrete NaCl-rich fluid ( $151\text{ mmol l}^{-1}$ ) when bathed in Ringer's solution containing  $3.4\text{ mmol l}^{-1} K^{+}$  (Hine et al., 2014). However, in the presence of  $34\text{ mmol l}^{-1} K^{+}$  (Fig. 8B), the tubules secrete a KCl-rich fluid like *D. melanogaster* Malpighian tubules (Hine et al., 2014). In parallel, the basolateral membrane voltage of 12 principal cells significantly depolarizes from  $-76.5 \pm 4.4$  to  $-41.2 \pm 1.7\text{ mV}$  ( $P < 10^{-6}$ ), similar to the depolarization of  $V_{bl}$  in *D. melanogaster* Malpighian tubules (Table 2), and the basolateral membrane resistance of principal cells significantly decreases from  $258.6 \pm 13.6$  to  $165.2 \pm 9.2\text{ k}\Omega$  ( $P < 10^{-5}$ ) in the same cells. Thus, Malpighian

tubules of both *A. aegypti* and *D. melanogaster* respond to peritubular  $Na^{+}$  by increasing transepithelial  $Na^{+}$  secretion at the expense of  $K^{+}$  secretion, and respond to peritubular  $K^{+}$  by increasing transepithelial  $K^{+}$  secretion at the expense of  $Na^{+}$  secretion (Fig. 8). The tubules do so spontaneously *in vitro* without signalling by extracellular natriuretic or kaliuretic agents. *Aedes aegypti* evolved 189 million years after *D. melanogaster*. Thus it appears that the capacity for secreting  $K^{+}$  and  $Na^{+}$  by *D. melanogaster* Malpighian tubules has allowed females of *A. aegypti* to adopt hematophagous habits and to excrete the  $Na^{+}$  load of blood meals because their Malpighian tubules have retained ancestral mechanisms.

### Acknowledgements

Thanks are due to Frederike Schöne and Laura Momann for the study of *Aedes aegypti* Malpighian tubules in  $34\text{ mmol l}^{-1} K^{+}$  Ringer's solution; Leonard Breitsprecher for providing the image in Fig. 1; Dr Heiko Harten and Prof. Dr Achim Paululat for providing *Drosophila melanogaster*; and the University of Osnabrück for providing space and equipment under the auspices of my guest professorship in the Department of Biology/Chemistry.

### Competing interests

The author declares no competing or financial interests.

### Funding

This research received no specific grant from any funding agency in the public, commercial or not-for-profit sectors.

### References

- Bello-Reuss, E., Grady, T. P. and Reuss, L. (1981). Mechanism of the effect of cyanide on cell membrane potentials in *Necturus* gall-bladder epithelium. *J. Physiol.* **314**, 343–357. doi:10.1113/jphysiol.1981.sp013712
- Beyenbach, K. W. (1993a). Extracellular fluid homeostasis in insects? In *Molecular Comparative Physiology*, Vol. 12 (ed. R. H. K. Kinne, E. Kinne-Saffran and K. W. Beyenbach), pp. 146–173. Basel: Karger.
- Beyenbach, K. W. (1993b). *Structure and Function of Primary Messengers in Invertebrates: Insect Diuretic and Antidiuretic Peptides*. Basel; New York: Karger.
- Beyenbach, K. W. (2003). Transport mechanisms of diuresis in Malpighian tubules of insects. *J. Exp. Biol.* **206**, 3845–3856. doi:10.1242/jeb.00639
- Beyenbach, K. W. (2012). A dynamic paracellular pathway serves diuresis in mosquito Malpighian tubules. *Ann. N. Y. Acad. Sci.* **1258**, 166–176. doi:10.1111/j.1749-6632.2012.06527.x
- Beyenbach, K. W. (2016). The plasticity of extracellular fluid homeostasis in insects. *J. Exp. Biol.* **219**, 2596–2607. doi:10.1242/jeb.129650
- Beyenbach, K. W. and Masia, R. (2002). Membrane conductances of principal cells in Malpighian tubules of *Aedes aegypti*. *J. Insect Physiol.* **48**, 375–386. doi:10.1016/S0022-1910(02)00057-4
- Beyenbach, K. W. and Petzel, D. H. (1987). Diuresis in mosquitoes: role of a natriuretic factor. *News Physiol. Sci.* **2**, 171–175. doi:10.1152/physiologyonline.1987.2.5.171
- Beyenbach, K. W. and Piermarini, P. M. (2011). Transcellular and paracellular pathways of transepithelial fluid secretion in Malpighian (renal) tubules of the yellow fever mosquito *Aedes aegypti*. *Acta Physiol. (Oxf.)* **202**, 387–407. doi:10.1111/j.1748-1716.2010.02195.x
- Beyenbach, K. W. and Wiczorek, H. (2006). The V-type  $H^{+}$  ATPase: molecular structure and function, physiological roles and regulation. *J. Exp. Biol.* **209**, 577–589. doi:10.1242/jeb.02014
- Beyenbach, K. W., Aneshansley, D. J., Pannabecker, T. L., Masia, R., Gray, D. and Yu, M.-J. (2000a). Oscillations of voltage and resistance in Malpighian tubules of *Aedes aegypti*. *J. Insect Physiol.* **46**, 321–333. doi:10.1016/S0022-1910(99)00185-7
- Beyenbach, K. W., Pannabecker, T. L. and Nagel, W. (2000b). Central role of the apical membrane  $H^{+}$ -ATPase in electrogenesis and epithelial transport in Malpighian tubules. *J. Exp. Biol.* **203**, 1459–1468.
- Blumenthal, E. M. (2001). Characterization of transepithelial oscillations in the *Drosophila* Malpighian tubule. *J. Exp. Biol.* **204**, 3075–3084.
- Blumenthal, E. M. (2003). Regulation of chloride permeability by endogenously produced tyramine in the *Drosophila* Malpighian tubule. *Am. J. Physiol. Cell Physiol.* **284**, C718–C728. doi:10.1152/ajpcell.00359.2002
- Boulpaep, E. L. and Giebisch, G. (1978). Electrophysiological measurements on the renal tubule. In *Methods in Pharmacology, Renal Pharmacology*, Vol. 4B (ed. M. Martinez-Maldonado), pp. 165–173. New York, NY: Springer US.

- Boulpaep, E. L. and Seely, J. F.** (1971). Electrophysiology of proximal and distal tubules in the autoperfused dog kidney. *Am. J. Physiol.* **221**, 1084–1096. doi:10.1152/ajplegacy.1971.221.4.1084
- Burg, M., Grantham, J., Abramow, M. and Orloff, J.** (1966). Preparation and study of fragments of single rabbit nephrons. *Am. J. Physiol.* **210**, 1293–1298. doi:10.1152/ajplegacy.1966.210.6.1293
- Cabrero, P., Richmond, L., Nitabach, M., Davies, S. A. and Dow, J. A. T.** (2013). A biogenic amine and a neuropeptide act identically: tyramine signals through calcium in *Drosophila* tubule stellate cells. *Proc. Biol. Sci.* **280**, 20122943. doi:10.1098/rspb.2012.2943
- Cabrero, P., Terhzaz, S., Romero, M. F., Davies, S. A., Blumenthal, E. M. and Dow, J. A. T.** (2014). Chloride channels in stellate cells are essential for uniquely high secretion rates in neuropeptide-stimulated *Drosophila* diuresis. *Proc. Natl. Acad. Sci. USA* **111**, 14301–14306. doi:10.1073/pnas.1412706111
- Chen, X.-G., Jiang, X., Gu, J., Xu, M., Wu, Y., Deng, Y., Zhang, C., Bonizzoni, M., Dermauw, W., Vontas, J. et al.** (2015). Genome sequence of the Asian Tiger mosquito, *Aedes albopictus*, reveals insights into its biology, genetics, and evolution. *Proc. Natl. Acad. Sci. USA* **112**, E5907–E5915. doi:10.1073/pnas.1516410112
- Davies, S. A., Huesmann, G. R., Maddrell, S. H., O'Donnell, M. J., Skaer, N. J., Dow, J. A. Tublitz, N. J.** (1995). CAP<sub>2b</sub>, a cardioacceleratory peptide, is present in *Drosophila* and stimulates tubule fluid secretion via cGMP. *Am. J. Physiol.* **269**, R1321–R1326. doi:10.1152/ajpregu.1995.269.6.r1321
- Denholm, B., Sudarsan, V., Pasalodos-Sanchez, S., Artero, R., Lawrence, P. A., Maddrell, S., Baylies, M. and Skaer, H.** (2003). Dual origin of the renal tubules in *Drosophila*: mesodermal cells integrate and polarize to establish secretory function. *Curr. Biol.* **13**, 1052–1057. doi:10.1016/S0960-9822(03)00375-0
- Dor'o, J. M.** (1968). Transport mechanisms in gall bladder. In *Handbook of Physiology*, Vol. 5, p. 2451. Washington, DC: American Physiological Society.
- Dow, J. A., Maddrell, S. H., Gortz, A., Skaer, N. J., Brogan, S. and Kaiser, K.** (1994). The Malpighian tubules of *Drosophila melanogaster*: a novel phenotype for studies of fluid secretion and its control. *J. Exp. Biol.* **197**, 421–428.
- Dow, J. A. T., Davies, S. A. and Sozen, M. A.** (1998). Fluid secretion by the *Drosophila* Malpighian tubule. *Am. Zool.* **38**, 450–460. doi:10.1093/icb/38.3.450
- Erlig, D.** (1976). Solute transport across isolated epithelia. *Kidney Int.* **9**, 76–87. doi:10.1038/ki.1976.13
- Frizzell, R. A. and Schultz, S. G.** (1972). Ionic conductances of extracellular shunt pathway in rabbit ileum. Influence of shunt on transmural sodium transport and electrical potential differences. *J. Gen. Physiol.* **59**, 318–346. doi:10.1085/jgp.59.3.318
- Frömter, E.** (1986). The electrophysiological analysis of tubular transport. *Kidney Int.* **30**, 216–228. doi:10.1038/ki.1986.174
- Halberg, K. A., Terhzaz, S., Cabrero, P., Davies, S. A. and Dow, J. A. T.** (2015). Tracing the evolutionary origins of insect renal function. *Nat. Commun.* **6**, 6800. doi:10.1038/ncomms7800
- Hegarty, J. L., Zhang, B., Pannabecker, T. L., Petzel, D. H., Baustian, M. D. and Beyenbach, K. W.** (1991). Dibutyl cAMP activates bumetanide-sensitive electrolyte transport in Malpighian tubules. *Am. J. Physiol. Cell Physiol.* **261**, C521–C529. doi:10.1152/ajpcell.1991.261.3.C521
- Hegel, U., Frömter, E. and Wick, T.** (1967). [Transmural electrical resistance of the proximal convoluted rat kidney tubule]. *Pflügers Arch. Gesamte Physiol. Menschen Tiere* **294**, 274–290. doi:10.1007/BF00363113
- Helman, S. I.** (1972). Determination of electrical resistance of the isolated cortical collecting tubule and its possible anatomical location. *Yale J. Biol. Med.* **45**, 339–345.
- Helman, S. I., Grantham, J. J. and Burg, M. B.** (1971). Effect of vasopressin on electrical resistance of renal cortical collecting tubules. *Am. J. Physiol.* **220**, 1825–1832. doi:10.1152/ajplegacy.1971.220.6.1825
- Hine, R. M., Rouhier, M. F., Park, S. T., Qi, Z., Piermarini, P. M. and Beyenbach, K. W.** (2014). The excretion of NaCl and KCl loads in mosquitoes. 1. Control data. *Am. J. Physiol. Regul. Integr. Comp. Physiol.* **307**, R837–R849. doi:10.1152/ajpregu.00105.2014
- Ianowski, J. P. and O'Donnell, M. J.** (2004). Basolateral ion transport mechanisms during fluid secretion by *Drosophila* Malpighian tubules: Na<sup>+</sup> recycling, Na<sup>+</sup>:K<sup>+</sup>:2Cl<sup>-</sup> cotransport and Cl<sup>-</sup> conductance. *J. Exp. Biol.* **207**, 2599–2609. doi:10.1242/jeb.01058
- Ianowski, J. P., Christensen, R. J. and O'Donnell, M. J.** (2004). Na<sup>+</sup> competes with K<sup>+</sup> in bumetanide-sensitive transport by Malpighian tubules of *Rhodnius prolixus*. *J. Exp. Biol.* **207**, 3707–3716. doi:10.1242/jeb.01203
- Jung, A. C., Denholm, B., Skaer, H. and Affolter, M.** (2005). Renal tubule development in *Drosophila*: a closer look at the cellular level. *J. Am. Soc. Nephrol.* **16**, 322–328. doi:10.1681/ASN.2004090729
- Linton, S. M. and O'Donnell, M. J.** (1999). Contributions of K<sup>+</sup>:Cl<sup>-</sup> cotransport and Na<sup>+</sup>/K<sup>+</sup>-ATPase to basolateral ion transport in Malpighian tubules of *Drosophila melanogaster*. *J. Exp. Biol.* **202**, 1561–1570.
- Lu, H.-L., Kersch, C. and Pietrantoni, P. V.** (2011). The kinin receptor is expressed in the Malpighian tubule stellate cells in the mosquito *Aedes aegypti* (L.): a new model needed to explain ion transport? *Insect Biochem. Mol. Biol.* **41**, 135–140. doi:10.1016/j.ibmb.2010.10.003
- Malnic, G. and Giebisch, G.** (1972). Some electrical properties of distal tubular epithelium in the rat. *Am. J. Physiol.* **223**, 797–808. doi:10.1152/ajplegacy.1972.223.4.797
- Miyauchi, J. T., Piermarini, P. M., Yang, J. D., Gilligan, D. M. and Beyenbach, K. W.** (2011). *The Role of Adducin in the Diuresis Triggered by Aedeskinin Iii in Malpighian Tubules of the Yellow Fever Mosquito*. Glasgow, Scotland: Society for Experimental Biology (SEB).
- Morgan, P. J. and Mordue, W.** (1981). Stimulated fluid secretion is sodium dependent in the Malpighian tubules of *Locusta migratoria*. *J. Insect Physiol.* **27**, 271–279. doi:10.1016/0022-1910(81)90061-5
- O'Connor, K. R. and Beyenbach, K. W.** (2001). Chloride channels in apical membrane patches of stellate cells of Malpighian tubules of *Aedes aegypti*. *J. Exp. Biol.* **204**, 367–378. doi:10.1007/978-1-4615-1321-6\_46
- O'Donnell, M. J. and Maddrell, S. H. P.** (1995). Fluid Reabsorption and ion transport by the lower malpighian tubules of adult female *Drosophila*. *J. Exp. Biol.* **198**, 1647–1653.
- O'Donnell, M. J., Dow, J. A., Huesmann, G. R., Tublitz, N. J. and Maddrell, S. H.** (1996). Separate control of anion and cation transport in Malpighian tubules of *Drosophila melanogaster*. *J. Exp. Biol.* **199**, 1163–1175.
- O'Donnell, M. J., Rheault, M. R., Davies, S. A., Rosay, P., Harvey, B. J., Maddrell, S. H., Kaiser, K. and Dow, J. A.** (1998). Hormonally controlled chloride movement across *Drosophila* tubules is via ion channels in stellate cells. *Am. J. Physiol.* **274**, R1039–R1049. doi:10.1152/ajpregu.1998.274.4.R1039
- Pannabecker, T. L., Aneshansley, D. J. and Beyenbach, K. W.** (1992). Unique electrophysiological effects of dinitrophenol in Malpighian tubules. *Am. J. Physiol.* **263**, R609–R614. doi:10.1152/ajpregu.1992.263.3.r609
- Pannabecker, T. L., Hayes, T. K. and Beyenbach, K. W.** (1993). Regulation of epithelial shunt conductance by the peptide leucokinin. *J. Membr. Biol.* **132**, 63–76. doi:10.1007/BF00233052
- Petzel, D. H.** (2000). Na<sup>+</sup>/H<sup>+</sup> exchange in mosquito Malpighian tubules. *Am. J. Physiol. Regul. Integr. Comp. Physiol.* **279**, R1996–R2003. doi:10.1152/ajpregu.2000.279.6.R1996
- Piermarini, P. M., Grogan, L. F., Lau, K., Wang, L. and Beyenbach, K. W.** (2010). A SLC4-like anion exchanger from renal tubules of the mosquito (*Aedes aegypti*): evidence for a novel role of stellate cells in diuretic fluid secretion. *Am. J. Physiol. Regul. Integr. Comp. Physiol.* **298**, R642–R660. doi:10.1152/ajpregu.00729.2009
- Piermarini, P. M., Hine, R. M., Schepel, M., Miyauchi, J. and Beyenbach, K. W.** (2011). Role of an apical K/Cl cotransporter in urine formation by renal tubules of the yellow fever mosquito (*Aedes aegypti*). *Am. J. Physiol. Regul. Integr. Comp. Physiol.* **301**, R1318–R1337. doi:10.1152/ajpregu.00223.2011
- Piermarini, P. M., Rouhier, M. F., Schepel, M., Kosse, C. and Beyenbach, K. W.** (2013). Cloning and functional characterization of inward-rectifying potassium (Kir) channels from Malpighian tubules of the mosquito *Aedes aegypti*. *Insect Biochem. Mol. Biol.* **43**, 75–90. doi:10.1016/j.ibmb.2012.09.009
- Piermarini, P. M., Dunemann, S. M., Rouhier, M. F., Calkins, T. L., Raphemot, R., Denton, J. S., Hine, R. M. and Beyenbach, K. W.** (2015). Localization and role of inward rectifier K(+) channels in Malpighian tubules of the yellow fever mosquito *Aedes aegypti*. *Insect Biochem. Mol. Biol.* **67**, 59–73. doi:10.1016/j.ibmb.2015.06.006
- Pilcher, D. E. M.** (1970). The influence of the diuretic hormone on the process of urine secretion by the Malpighian tubules of *Carausius morosus*. *J. Exp. Biol.* **53**, 465–484.
- Pugacheva, O. M. and Mamon, L. A.** (2003). [Genetic control of development of the Malpighian vessels in *Drosophila melanogaster*]. *Ontogenez* **34**, 325–341.
- Radford, J. C., Davies, S. A. and Dow, J. A. T.** (2002). Systematic G-protein-coupled receptor analysis in *Drosophila melanogaster* identifies a leucokinin receptor with novel roles. *J. Biol. Chem.* **277**, 38810–38817. doi:10.1074/jbc.M203694200
- Radford, J. C., Terhzaz, S., Cabrero, P., Davies, S.-A. and Dow, J. A.** (2004). Functional characterisation of the *Anopheles* leucokinin and their cognate G-protein coupled receptor. *J. Exp. Biol.* **207**, 4573–4586. doi:10.1242/jeb.01317
- Reuss, L. and Finn, A. L.** (1974). Passive electrical properties of toad urinary bladder epithelium. Intercellular electrical coupling and transepithelial cellular and shunt conductances. *J. Gen. Physiol.* **64**, 1–25. doi:10.1085/jgp.64.1.1
- Rheault, M. K. and O'Donnell, M. J.** (2001). Analysis of epithelial K<sup>+</sup> transport in Malpighian tubules of *Drosophila melanogaster*: evidence for spatial and temporal heterogeneity. *J. Exp. Biol.* **204**, 2289–2299.
- Rheault, M. R. and O'Donnell, M. J.** (2004). Organic cation transport by Malpighian tubules of *Drosophila melanogaster*: application of two novel electrophysiological methods. *J. Exp. Biol.* **207**, 2173–2184. doi:10.1242/jeb.01003
- Rheault, M. R., Okech, B. A., Keen, S. B. W., Miller, M. M., Meleshkevitch, E. A., Linsler, P. J., Boudko, D. Y. and Harvey, K. W.** (2007). Molecular cloning, phylogeny and localization of AgNHA1: the first Na<sup>+</sup>/H<sup>+</sup> antiporter (NHA) from a metazoan, *Anopheles gambiae*. *J. Exp. Biol.* **210**, 3848–3861. doi:10.1242/jeb.007872
- Rodan, A. R., Baum, M. and Huang, C.-L.** (2012). The *Drosophila* NKCC Ncc69 is required for normal renal tubule function. *Am. J. Physiol. Cell Physiol.* **303**, C883–C894. doi:10.1152/ajpcell.00201.2012



- Schellinger, J. N. and Rodan, A. R. (2015). Use of the Ramsay assay to measure fluid secretion and ion flux rates in the *Drosophila melanogaster* Malpighian tubule. *J. Vis. Exp.* **105**, 52968-52972. doi:10.3791/53144
- Schepel, S. A., Fox, A. J., Miyauchi, J. T., Sou, T., Yang, J. D., Lau, K., Blum, A. W., Nicholson, L. K., Tiburcy, F., Nachman, R. J. et al. (2010). The single kinin receptor signals to separate and independent physiological pathways in Malpighian tubules of the yellow fever mosquito. *Am. J. Physiol. Regul. Integr. Comp. Physiol.* **299**, R612-R622. doi:10.1152/ajpregu.00068.2010
- Singh, S. R., Liu, W. and Hou, S. X. (2007). The adult *Drosophila* malpighian tubules are maintained by multipotent stem cells. *Cell Stem Cell* **1**, 191-203. doi:10.1016/j.stem.2007.07.003
- Sozen, M. A., Armstrong, J. D., Yang, M., Kaiser, K. and Dow, J. A. T. (1997). Functional domains are specified to single-cell resolution in a *Drosophila* epithelium. *Proc. Natl. Acad. Sci. USA* **94**, 5207-5212. doi:10.1073/pnas.94.10.5207
- Spring, K. R. and Paganelli, C. V. (1972). Sodium flux in *Necturus* proximal tubule under voltage clamp. *J. Gen. Physiol.* **60**, 181-201. doi:10.1085/jgp.60.2.181
- Taylor, R. E. (1963). Cable theory. In *Physical Techniques in Biological Research*, Vol. VI/B (ed. W. L. Nastuk), pp. 219-262. New York, NY: Academic Press.
- Terhzaz, S., O'Connell, F. C., Pollock, V. P., Kean, L., Davies, S. A., Veenstra, J. A. and Dow, J. A. T. (1999). Isolation and characterization of a leucokinin-like peptide of *Drosophila melanogaster*. *J. Exp. Biol.* **202**, 3667-3676.
- Tiburcy, F., Beyenbach, K. W. and Wiczorek, H. (2013). Protein kinase A-dependent and -independent activation of the V-ATPase in Malpighian tubules of *Aedes aegypti*. *J. Exp. Biol.* **216**, 881-891. doi:10.1242/jeb.078360
- Ussing, H. H. and Windhager, E. E. (1964). Nature of shunt path and active sodium transport path through frog skin epithelium. *Acta Physiol. Scand.* **61**, 484-504.
- Weng, X.-H., Huss, M., Wiczorek, H. and Beyenbach, K. W. (2003). The V-type H<sup>+</sup>-ATPase in Malpighian tubules of *Aedes aegypti*: localization and activity. *J. Exp. Biol.* **206**, 2211-2219. doi:10.1242/jeb.00385
- Weng, X.-H., Piermarini, P. M., Yamahiro, A., Yu, M.-J., Aneshansley, D. J. and Beyenbach, K. W. (2008). Gap junctions in Malpighian tubules of *Aedes aegypti*. *J. Exp. Biol.* **211**, 409-422. doi:10.1242/jeb.011213
- Williams, J. C. and Beyenbach, K. W. (1983). Differential effects of secretagogues on Na and K secretion in the Malpighian tubules of *Aedes aegypti* (L.). *J. Comp. Physiol.* **149**, 511-517. doi:10.1007/BF00690010
- Williams, J. C. and Beyenbach, K. W. (1984). Differential effects of secretagogues on the electrophysiology of the Malpighian tubules of the yellow fever mosquito. *J. Comp. Physiol. B* **154**, 301-309. doi:10.1007/BF02464411
- Wright, E. M. (1972). Mechanisms of ion transport across the choroid plexus. *J. Physiol.* **226**, 545-571. doi:10.1113/jphysiol.1972.sp009997
- Wu, D. S. and Beyenbach, K. W. (2003). The dependence of electrical transport pathways in Malpighian tubules on ATP. *J. Exp. Biol.* **206**, 233-243. doi:10.1242/jeb.00066
- Wu, Y., Baum, M., Huang, C.-L. and Rodan, A. R. (2015). Two inwardly rectifying potassium channels, Irk1 and Irk2, play redundant roles in *Drosophila* renal tubule function. *Am. J. Physiol. Regul. Integr. Comp. Physiol.* **309**, R747-R756. doi:10.1152/ajpregu.00148.2015
- Xiang, M. A., Linser, P. J., Price, D. A. and Harvey, W. R. (2012). Localization of two Na<sup>+</sup>- or K<sup>+</sup>-H<sup>+</sup> antiporters, AgNHA1 and AgNHA2, in *Anopheles gambiae* larval Malpighian tubules and the functional expression of AgNHA2 in yeast. *J. Insect Physiol.* **58**, 570-579. doi:10.1016/j.jinsphys.2011.12.009
- Yu, M.-J. and Beyenbach, K. W. (2001). Leucokinin and the modulation of the shunt pathway in Malpighian tubules. *J. Insect Physiol.* **47**, 263-276. doi:10.1016/S0022-1910(00)00084-6
- Yu, M.-J. and Beyenbach, K. W. (2002). Leucokinin activates Ca<sup>2+</sup>-dependent signal pathway in principal cells of *Aedes aegypti* Malpighian tubules. *Am. J. Physiol. Renal. Physiol.* **283**, F499-F508. doi:10.1152/ajprenal.00041.2002